

SURFACE QUALITY AND FABRICATION DIRECTIONALITY EFFECTS ON THE FATIGUE BEHAVIOR OF DMLS Ti6Al4V

FRKÁŇ Martin¹, KONEČNÁ Radomila¹, NICOLETTO Gianni²

¹University of Žilina, Department of Materials Engineering, Žilina, Slovakia, EU
martin.frkan@fstroj.uniza.sk, radomila.konecna@fstroj.uniza.sk

²University of Parma, Department of Engineering and Architecture, Parma, Italy, EU
gianni.nicoletto@unipr.it

Abstract

Direct Metal Laser Sintering (DMLS), one of Additive Manufacturing technologies, produces layer-by-layer geometrically complex components from metal powders, such as nickel alloys, titanium alloys, aluminum alloys, etc. using a high power concentrated laser beam. The material structure created by this technology is influenced by process parameters and build orientation. The process is characterized by localized high heat inputs during very short interaction times leading to the formation of very fine structures but also to the generation of internal stresses. Therefore, the DMLS parts are heat treated to decrease or completely remove residual stresses. The DMLS manufacturing process examined here was characterized by a 400 W laser power and 60 µm layer thickness applied to a fine Ti6Al4V powder. Plane bending fatigue testing was performed on three sets of special miniature specimens prepared according to three different build orientations. A cyclic bending stress was applied to the smooth flat surface of the specimens. The surface was tested in the as-built state and in the polished state to reduce roughness of the as-built surface. The fatigue behavior of DMLS Ti6Al4V was found to be influenced by the build orientation. Fatigue specimens with polished surfaces showed better fatigue properties compared to the as-built specimens.

Keywords: Ti6Al4V, DMLS, fatigue, microstructure

1. INTRODUCTION

Additive Manufacturing (AM) is an innovative process allowing the production directly from a CAD model of near-net shape parts that otherwise are impossible to produce by conventional procedures. AM is a primary manufacturing technology when the shape of the part is complex and conventional post machining is limited to only few functional details, such as threads or high-finish areas. Therefore, AM is used in many different sectors, such as medical, aerospace, automotive, prototyping and others. The number of applications of this technology is steadily growing as the AM capabilities are increasingly accepted [1, 2, 3].

Direct Metal Laser Sintering (DMLS) is a common Powder-Bed-Fusion (PBF) process for fabricating parts from metal powders, such as aluminum, nickel, steel and titanium. In this process, a metal base plate is used for supporting the parts during the layer-by-layer building process, where a thin layer of metal powder is repeatedly spread and selectively melted by a laser beam. The scanning area of the laser at each layer is obtained from the CAD file of the part. After each laser scanning phase, the base plate is lowered in the Z-direction of one-layer thickness to allow recoating. This coating/melting process repeats itself until the part is completed [4, 5, 6].

The study deals with analysis of the specimens prepared by DMLS. This technology involves a lot of variables, such as laser power, layer thickness, scanning strategy and more. All these variables have significantly effect on the mechanical properties of the specimens. Years of research have optimized these parameters to achieve the best properties. Furthermore, the research has focused on post fabrication heat treatments in consideration of that internal stresses arise in the solidified material because of high cooling rates [7, 8]. This paper reports

the investigation of microstructure, basic mechanical properties and fatigue behavior of specimens after a specific stress-relieving heat treatment.

2. EXPERIMENTS

Specimens were manufactured using the Ti64 powder (Ti6Al4V alloy) supplied by EOS GmbH. The powder particles were spherical with a predominant diameter range from 25 to 45 μm and with a chemical composition given in **Table 1**.

Table 1 Chemical composition of Ti64 powder (wt.%)

	Al	V	O	N	H	Fe	C	Ti
Standard value	5.5-6.5	3.5-4.5	< 0.1	< 0.05	< 0.012	< 0.25	< 0.08	bal.
Actual value	6.29	4.07	0.091	0.005	0.002	0.22	0.005	bal.

The specimens were manufactured using the DMLS technology on EOS M280 machine. This system uses Yb fiber laser unit with a wavelength of 1075 nm, which is able to supply laser power of 200 W or 400 W. EOS M280 is equipped with building chamber filled with Ar gas to avoid oxidation of titanium powder. The manufacturing process of specimens used 400 W laser power and 60 μm layer thickness. After fabrication, a specific heat treatment was used to decrease internal stresses. Parameters of heat treatment cannot be specified.

The microstructure was observed using a light optical microscope Zeiss Axio Observer Z1M on polished and etched (10% HF for 10 s) samples that were cut from the fatigue testing specimens. Observation of structure was made in order to characterize material anisotropy, which arise by the typical process conditions, (i.e. layer-by-layer generative principle, short interactions, high temperature gradients and the high localization of this manufacturing process). Fracture surfaces were examined in a SEM Tescan VEGA LMU II. Vickers hardness tests were performed on polished specimens using HPO 250/AQ machine with a load of 10 N and 10 s of loading time. Surface roughness was measured in the longitudinal direction on the flat plane subjected to cyclic tensile loading on a Mitutoyo SJ 210 machine.

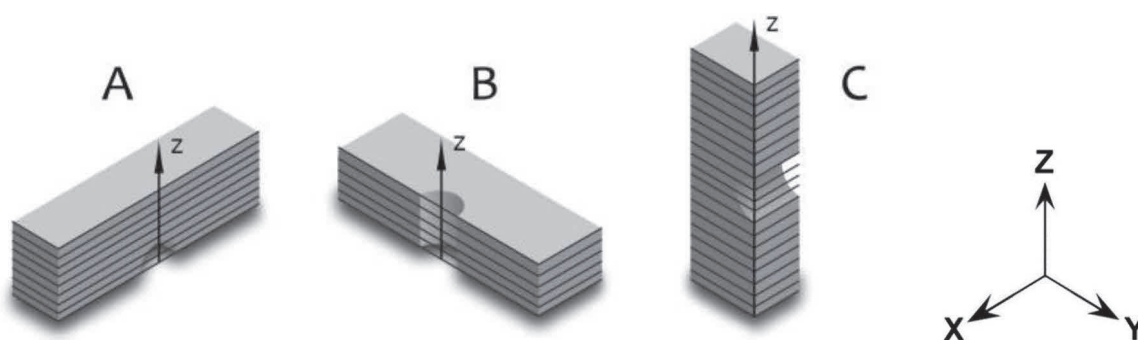


Figure 1 Denomination of fatigue specimens and their different build orientations

Fatigue testing was performed at room temperature on a Schenk-type plane bending fatigue testing machine. A loading cycle was sinusoidal with a frequency $f = 15$ Hz and loading cycle asymmetry was $R = 0$. Special miniature specimens $5 \times 5 \pm 0.2$ mm in minimum cross-section and 22 ± 0.2 mm in length as shown in **Figure 1**, were used for fatigue testing [9]. The aim of the specimen design was the minimization of material required for manufacturing and the generation of three specimen orientations in the as-built condition. The flat surface was under cyclic loading. The round notch was created to control crack initiation in the middle region of specimens. To investigate the role of surface roughness, some specimens were tested in an as-built condition and others

in a manually ground condition. The manual dry grinding process was performed using two SiC abrasive papers: initially a rough (grit size 500) paper and then a fine (grit size 1000) paper.

3. RESULTS AND DISCUSSION

Tensile tests were carried out on specimens fabricated in horizontal orientations (C orientation in **Figure 1**). The corresponding tensile test results are shown in **Table 2**. The tensile properties (ultimate tensile strength, yield strength) are comparable to the standard Ti64 cast and annealed material [10]. However, the specimens built by DMLS process have reached higher value of elongation.

Table 2 Mechanical properties

Material	R_m (MPa)	$R_{p0.2}$ (MPa)	A (%)	E (GPa)
Ti64 DMLS - as-built + HT	954	840	18	118.145
Ti64 - cast + annealed	930	885	13	

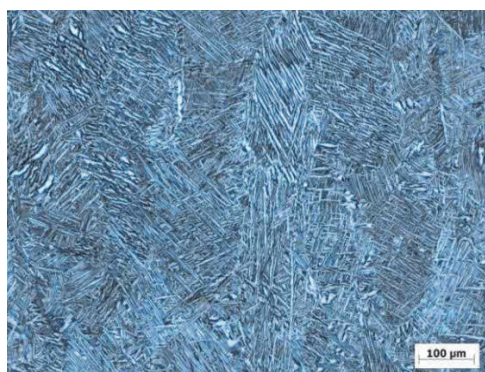
Surface roughness. Average values of surface roughness under the loading are shown in **Table 3**. From the measured values is visible that the values of the roughness depend on the building orientation of the specimens. The ground specimens A and C showed the same roughness value and lower than in as-built state.

Table 3 Surface roughness of the plane under the loading (see **Figure 1**)

Roughness	Direction A	Direction B	Direction C	After grinding A and C
R_a (μm)	3.3	13.1	13.4	0.18
R_z (μm)	20.1	88.8	80.6	1.44

Hardness of specimens was in all cases similar and the average value of hardness was 350 HV10.

Microstructural analysis of specimens after heat treatment (**Figure 2**) showed a two-phase structure formed by the $\alpha+\beta$ phases. The analysis was performed on three perpendicular planes due to the formation of the texture in this manufacturing process. Differences were observed between the lateral planes and the perpendicular plane to the build direction. Lateral planes (**Figures 2a, b**) show texture characterized by prior columnar grains of β -phase. These columnar grains have a length of several building layers and they were oriented parallel to the build direction. The perpendicular plane (**Figure 2c**) showed the cross-sections of these primary β columnar grains that appear as regular polyhedral grains. The size of these grains corresponded to the width of the columnar grains.



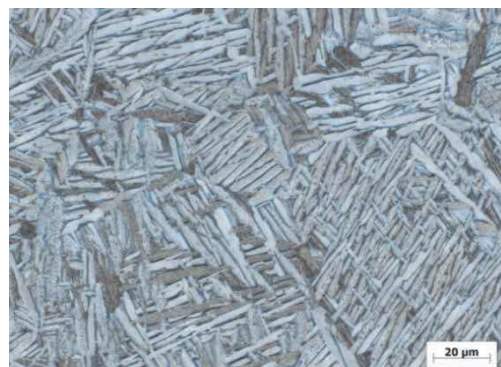
a) lateral X-Z plane



b) lateral Y-Z plane



c) orthogonal X-Y plane



d) microstructure detail, X-Y plane

Figure 2 Microstructure of stress relieved Ti6Al4V specimen prepared by DMLS

The β columnar grains were filled with lamellas of $\alpha+\beta$ phases, which were locally arranged in the Widmanstätten form. The thickness of the $\alpha+\beta$ lamellas was different and depended on the orientation of the lamellas to the metallographic section. Locally, a small amount of the coarsening α -phase grains was observed. Defects in the form of relatively large microshrinkages were only locally observed.

Fatigue tests results are shown in the form of S-N curves (**Figure 3**). All three specimens' orientations (A, B, C) were tested in as-built and heat treated state. Only orientations A and C of the ground specimens were tested as the specimens A and B in as-built state showed very similar fatigue behavior and grinding are not expected to introduce an influence.

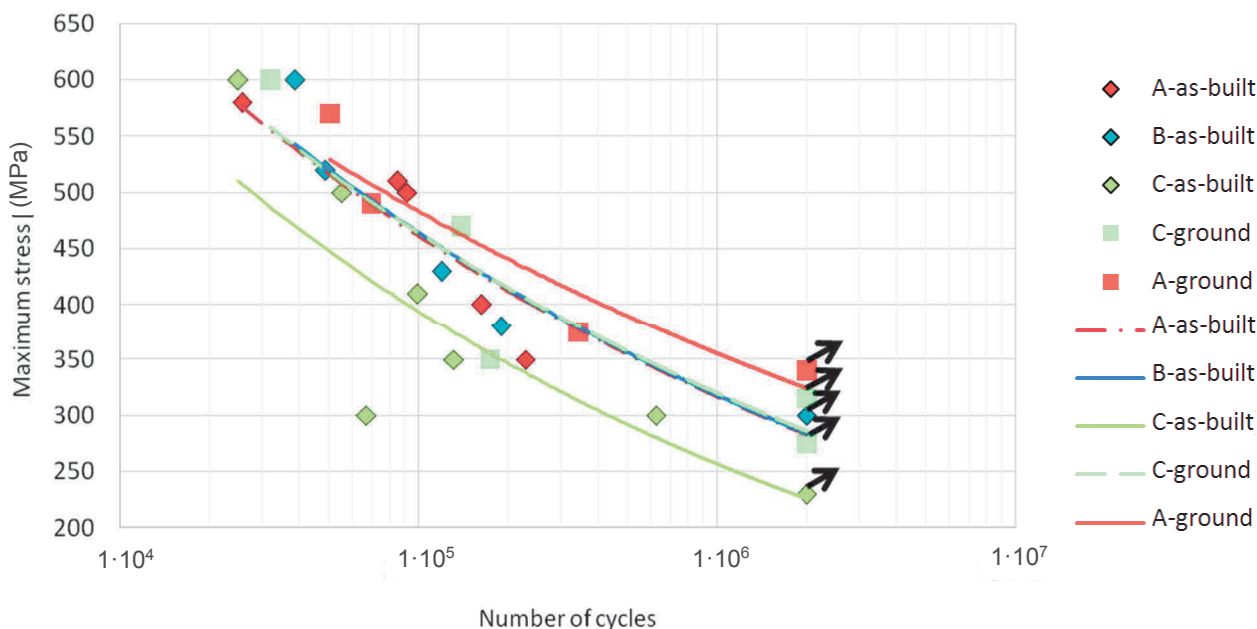


Figure 3 S-N curves of DMLS Ti6Al4V specimens in as-built and ground states

As shown by the microstructures (**Figure 2**) all specimens were identical. The orientation of material texture to the loading, which depends on building orientation, has a similar influence on the fatigue behavior in as-built state and ground state. The S-N curves in **Figure 3** show also the significant effect of specimen building orientation on the fatigue life. For specimens in as-built state with A and B orientations, S-N curves showed similar fatigue properties. They achieve longer fatigue lives in comparison to the specimens with C orientation. The ground specimens also showed influence of the building orientation on the fatigue life, but the differences

between specimens A and C in ground state are not as significant as in the case of the specimens in the as-built state. According these results the influence of the building orientation on fatigue life is present for both surface states.

Differences in fatigue behavior between as-built and ground state were related to the roughness of the planes under loading. From the comparison of as-built and ground specimens, the fatigue life is longer for the specimens with a ground surface. The positive effect of grinding is more significant for the specimens with building orientation C. The fatigue life of ground specimens with this orientation increased and reached a level of as-built specimens with orientation A and B as it is shown in **Figure 3**.

The present fatigue results for the Ti64 alloy show differences when we compare to the fatigue data published in the paper [11] where the same material powder and DMLS process parameters were used but a different post fabrication heat treatment was performed on the specimens. The influence of build orientation tested in [11] did not exhibit the similar effect. The fatigue data of [11] showed a small scatter in dependence of specimen orientation. The different parameters of stress relieving heat treatment resulted in different microstructures: fine α -phase needles in the β matrix in [11] and lamellar $\alpha+\beta$ microstructure here.

Fractography analysis. Fracture surfaces of selected fatigue specimens are shown in **Figure 4**. In general, the process of fatigue fracture is characterized by the crack initiation (**Figure 4b**), crack propagation (**Figure 4c**) and final fracture (**Figure 4d**). In the present tests, fatigue crack initiation has always started on the surface of the specimen due to the bending loading and also due to the surface condition associated with the manufacturing process. Differences were seen in specimens loaded at low and at high stress levels. Specimens subjected to low cyclic stress showed one initiating place, while specimens loaded at high stresses exhibited multiple initiations. In the case of as-built specimens, the crack initiated from the corner of the specimens (stress concentrator) or from non-melted particles. For ground specimens, the crack initiation started always from corner of the specimens. The area of crack propagation (**Figure 4c**) was similar for all specimens and characterized by a transcrystalline fatigue fracture. The typical sign of fatigue fracture (striations) were observed on fatigue fracture areas. The final rupture was characterized by the transcrystalline ductile fracture with dimple morphology (**Figure 4d**).

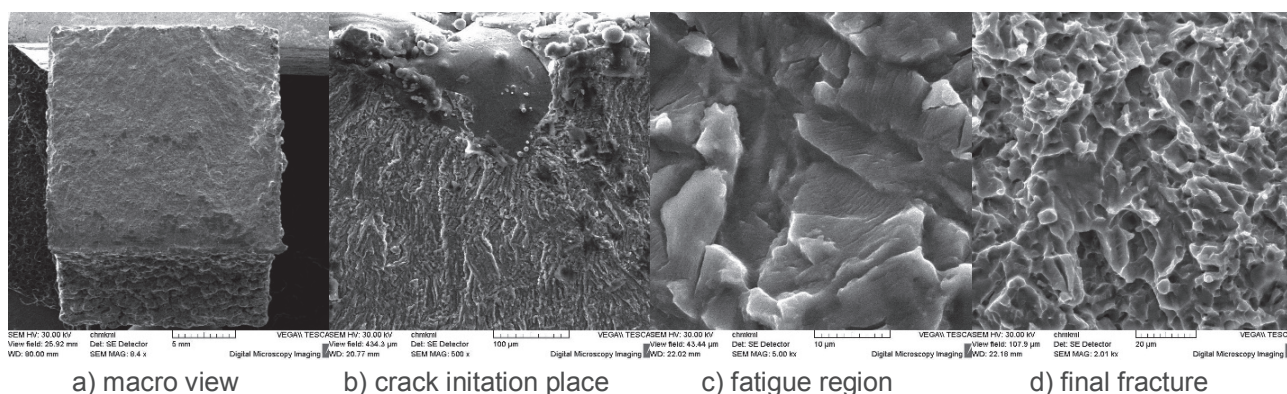


Figure 4 Fatigue fracture surface characterization, SEM

4. CONCLUSIONS

- The microstructure of Ti6Al4V prepared by DMLS and post fabrication heat treated showed $\alpha+\beta$ lamellar microstructure.
- The effect of build orientation on fatigue behavior was found to be significant for as-built specimens and also for ground specimens.

- Grinding decreases the influence of build orientation on the fatigue behavior and increase the fatigue life compared to the as-built condition.
- In the case of as-built specimens the crack initiation started from the corner of the specimens or from the non-melted particles. For ground specimens crack initiations were always at specimen corners.
- The mechanism of fatigue crack propagation was similar for all specimens and characterized by a transcrystalline fatigue fracture with striations.
- The final fracture was characterized by the transcrystalline ductile micromechanism with dimple morphology.

ACKNOWLEDGEMENTS

The research was supported by the Slovak VEGA grant No. 1/0685/2015. Specimen production by Beam-It, Forno Taro (Italy) is acknowledged with thanks.

REFERENCES

- [1] BANDYOPADHYAY, A., BOSE, A. *Additive manufacturing: Additive manufacturing technologies of metals using powder-based technology*. Taylor & Francis Group: Boca Raton, 2016, 377 p.
- [2] GEBHARDT, A. *Understanding additive manufacturing: Rapid prototyping, Rapid tooling, Rapid manufacturing*. Hanser Publishers: Munich, 2011, 173 p.
- [3] GIBSON, I., ROSEN, D., STUCKER, B. *Additive manufacturing technologies: 3D printing, rapid prototyping, and direct digital manufacturing*. Springer: New York, 2015, 498 p.
- [4] GONG, H., RAFI, K., STARR, T., STUCKER, B. The effects of processing parameters on defect regularity in Ti-6Al-4V parts fabricated by selective laser melting and electron beam melting. In *24th Annual International Solid Freeform Fabrication Symposium*. 2013, pp. 424-439.
- [5] SIMONELLI, M., TSE, Y. Y., TUCK, C. Further understanding of Ti-6Al-4V selective laser melting using texture analysis. In *23rd Annual International Solid Freeform Fabrication Symposium*. 2012, pp. 480-491.
- [6] SRIVATSAN, T. S., SUDARSHAN, T. S. *Additive manufacturing: Innovations, advances, and applications*. Taylor & Francis Group : Boca Raton, 2016, 444 p.
- [7] KNOWLES, C. R., BECKER, T. H., TAIT, R. B. Residual stress measurements and structural integrity implications for selective laser melted Ti-6Al-4V. *Journal of Industrial Engineering*, 2012, vol. 23, no. 3, pp. 119-129.
- [8] SHIOMI, M., OSAKADA, K., NAKAMURA, K., YAMASHITA, T., ABE, F. Residual stress within metallic model made by selective laser melting process. *Journal of the CIRP Annals - Manufacturing Technology*, 2004, vol. 53, no. 1, pp. 195-198.
- [9] NICOLETTO, G. Anisotropic high cycle fatigue behavior of Ti-6Al-4V obtained by powder bed laser fusion. *International Journal of Fatigue*, 2016, vol. 94, pp. 255-262.
- [10] *Properties and selection: Nonferrous alloys and special-purpose materials*. ASM International: 1990, vol. 2, 1328 p.
- [11] BAČA, A., KONEČNÁ, R., NICOLETTO, G. Influence of the direct metal laser sintering process on the fatigue behavior of the Ti6Al4V alloy. 2017 (in print).